Article:

Lu, H., Zeng, X. orcid.org/0000-0003-4896-8080, Ungar, G. orcid.org/0000-0002-9743-2656 et al. (2 more authors) (2018) The solution of the puzzle of smectic-Q: The phase structure and the origin of spontaneous chirality. Angewandte Chemie, 130 (11). pp. 2885-2890. ISSN 0044-8249

https://doi.org/10.1002/ange.201712812

This is the peer reviewed version of the following article: H. Lu, X. Zeng, G. Ungar, C. Dressel, C. Tschierske, The Solution of the Puzzle of Smectic-Q: The Phase Structure and the Origin of Spontaneous Chirality, Angew. Chem. 2018, 130(11), 2885-2890, which has been published in final form at https://doi.org/10.1002/ange.201712812. This article may be used for non-commercial purposes in accordance with Wiley Terms and Conditions for Use of Self-Archived Versions.

Solution of the Puzzle of Smectic-Q: The Phase Structure and the Origin of Spontaneous Chirality

Huanjun Lu,[a] Xiangbing Zeng,*[a] Goran Ungar,*[a,b] Christian Dressel,[c] and Carsten Tschierske[c]

[a] H. Lu, X. B. Zeng and G. Ungar, Department of Materials Science and Engineering, Sheffield University, Sheffield S1 3JD, UK, x.zeng@sheffield.ac.uk

[b] G. Ungar, Department of Physics, Zhejiang Sci-Tech University, Xiasha College Park, Hangzhou 310018, China, g.ungar@sheffield.ac.uk

[c] C. Dressel and C. Tschierske, Institute of Chemistry, Organic Chemistry, Martin-Luther-University Halle-Wittenberg, Kurt-Mothes-Str.2, 06120 Halle, Germany, carsten.tschierske@chemie.uni-halle.de

Abstract

The so-called Smectic-Q phase (SmQ) liquid crystal phase has been discovered in 1983 in rod-like molecules, but its structure remain unclear in spite of numerous attempts to solve it. Here we report what we believe to be the solution: a unique bicontinuous phase that is non-cubic and is made up of orthogonal twisted columns with planar 4-way junctions. While previously SmQ had only been seen in chiral compounds, here we show that this chiral phase forms also in achiral materials through spontaneous symmetry breaking. The results strongly support the idea of helical substructure of bicontinuous phases and long-range homochirality being sustained by helicity-matching at network junctions. The model also explains the triangular shape of double-gyroid domains growing within a SmQ environment. SmQ-forming materials hold potential for applications such as circularly polarized light emitters, requiring no alignment or asymmetric synthesis.

Text

Liquid crystals (LC) encompass a wide range of phases, from the simplest nematic, used in most displays, to those with structures of extraordinary complexity. Such complex structures are of considerable interest for nanotechnology in their own right, but they also have parallels in other soft matter. The transfer of knowledge on cubic phases from lyotropic liquid crystals (LC)[1] to block copolymers[2] is well documented. Also, in a number of cases new complex structures have first been found and understood in *thermotropic* (neat) LCs,[3,4] and then replicated in block copolymers,[5,6,7] lyotropics.[8] or other mesoscale systems.[9] Determining such structures can involve intricate detective work, but a solution is usually found relatively soon after their discovery. One notable exception is the so-called Smectic-Q (SmQ) phase, which has puzzled researchers ever since it was discovered in 1983.[10]

Since its initial discovery, SmQ phase has been reported and discussed several times in chiral compounds. In most cases such molecules consisted of an aromatic rod-like core with two identical chiral end-chains attached, one at each end.[10,11] SmQ is very sensitive to enantiomeric purity, and has so far only been observed in pure or nearly pure enantiomers. The phase is normally observed immediately below the isotropic liquid (Iso) phase, and on further cooling it was found to transform to the antiferroelectric smectic-C phase (SmC*$_A$). The unit cell height is also similar to the two-layer period in SmC*$_A$. On this basis, SmQ has been considered as a complex organization of small layer-like SmC*$_A$ grains,[11] as a result of the conflict between the tendencies for the chiral molecules to twist and, at the same time, form flat smectic layers.

With the help of single domain X-ray diffraction, the space group of the SmQ phase has been determined unequivocally as $I4_122$.[12] Using diffraction intensities, the validity of certain geometric models have also been analysed more quantitatively.[12] In a recent attempt[13] the model suggested in ref. [12] was further modified based on electron density maps. However, the proposed models still fail to rationalize adequately the existence of the SmQ phase, its structural chirality, and how its existence is linked to the intrinsic chirality of the molecules.

While SmQ is observed in enantiopure compounds, the $Ia\bar{3}d$ (Gyroid) bicontinuous cubic (Cub$_{bi}$) phase is often observed in their racemic mixtures,[11] or in compounds with the two end chains having opposite chiralities.[13] It has been pointed out[14] that by making chiral the Cub$_{bi}$ structures, the resulting lattices distort to tetragonal with different symmetries, including that of SmQ ($I4_122$). Tetragonal distortion of the $Ia\bar{3}d$ cubic, albeit to a $I4_1/acd$ symmetry, has been reported for a racemic mixture, adding support to such a connection between $Ia\bar{3}d$ and SmQ structures.[15] Another commonly observed phase in such compounds is the triple-network cubic phase,[16] which has recently been found to be chiral and can form in both chiral and achiral compounds, in the latter through dynamic mirror symmetry breaking.[17] Its space group has formerly been assigned as $Im\bar{3}m$ in achiral compounds, but has recently sometimes also been referred to as $I432$, because of its chirality; the question of its true space group symmetry is still open. It has also been reported that, starting from what appears to be an achiral triple-network cubic phase in a racemate, by increasing enantiomeric excess a phase transition to SmQ is observed.[18]

In the current work we report the observation of the chiral SmQ phase in *achiral* rod-like compounds, and present a new structural model showing SmQ to be a non-cubic bicontinuous phase formed by interwoven orthogonal helices, first of its kind.

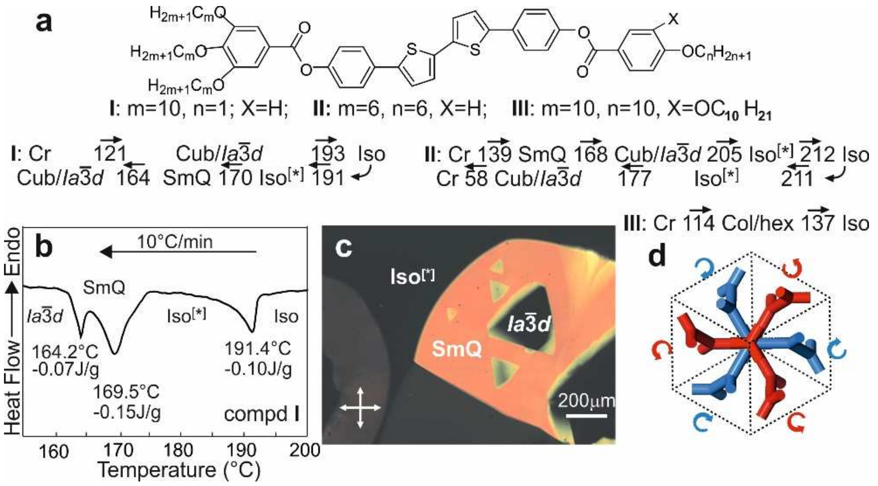

Figure 1. (a) Structure and phase transition temperatures (in °C) of compounds **I** – **III** (Cr = crystal, Iso$^{[*]}$ and Iso = chiral and achiral isotropic liquid). (b) DSC curve of **I** on cooling at 10 K/min. (c) Polarized optical micrograph of **I** in a 0.1 mm flat capillary at 164℃ after cooling from 200℃ at 10℃/min. The birefringent SmQ forms from Iso$^{[*]}$ and then transforms to cubic $Ia\bar{3}d$ within ~30 s. (d) Unit cell of Cub/$Ia\bar{3}d$ phase viewed along [111], to help explain triangular shape of SmQ domains growing within it; the two enantiomeric networks are shown in red and blue.

Compounds **I** - **III** and their mesophase sequence are shown in Fig. 1a. They belong to the series of achiral mesogens reported recently to form the achiral double-network $Ia\bar{3}d$ phase (Fig. 1d); through dynamic mirror symmetry breaking, they also form the chiral triple-network cubic phase, as well as the recently discovered chiral isotropic liquid (Iso$^{[*]}$) phase.[19]

The SmQ phase is found in **I** below ~169℃ on cooling at rates $\geq$10K/min from the Iso$^{[*]}$ which forms at ~191℃ (Fig. 1b). However, SmQ is metastable and quickly transforms to Cub/$Ia\bar{3}d$. This is illustrated in Fig. 1c, where SmQ domains (birefringent, yellow) emerging from the Iso$^{[*]}$ phase, are being replaced by Cub/$Ia\bar{3}d$ domains growing inside them. Crucially, the Cub/$Ia\bar{3}d$ domains have a triangular shape (trigonal prisms truncated by the film surface), with a 3-fold instead of 6-fold rotational symmetry expected from an achiral cubic phase viewed along [111] (Fig. 1d). This confirms the chirality of SmQ, as it acts as chiral environment breaking the degeneracy of growth rates of Cub/$Ia\bar{3}d$ domains along the six directions normal to its [111]. Due to the opposite hands of the two Cub/$Ia\bar{3}d$ networks, the chiral environment favours the growth of three of the six facets, the observed facets being the slow-growing ones. While examples of triangular chiral crystals exist,[20] we are not aware of examples of triangular non-chiral crystals or LCs.

In contrast to compound **I**, in **II** the SmQ forms on heating from solution-grown crystals, and is stable between 140℃ and ~168℃ (Fig. 1a). On cooling, a 30 K hysteresis is observed for the Iso$^{[*]}$-$Ia\bar{3}d$ transition, the origin of which will be discussed further below.

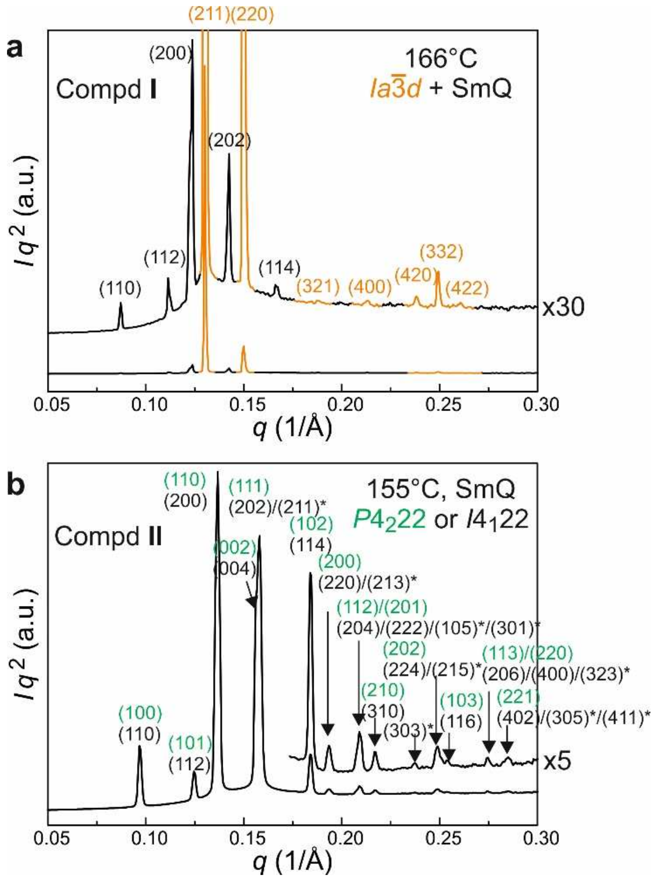

Figure 2. X-ray diffractograms of SmQ phase. (a) Mixture of Cub/$Ia\bar{3}d$ and SmQ in **I** at 166℃ after 50 K/min cooling from Iso. Indexed peaks of Cub/$Ia\bar{3}d$ and SmQ are orange and black, respectively. (b) Pure SmQ in compound **II**, recorded at 155℃ on heating. Indices on the smaller $P4_222$ and the full-size $I4_122$ unit cell are shown in green and black, respectively. Lattice parameters ($I4_122$): a=b=91.7Å, c=159.8Å. [*] marks *hkl* of peaks belonging to $I4_122$ only, and cannot be alternatively indexed on the $P4_222$ cell. Note the isolated (303)[*].

While at wider angles (4-5 Å) X-ray diffraction is only diffuse, at small angles a series of sharp Bragg peaks are seen for the SmQ in compounds **I** and **II** (Fig. 2). In both cases they can be indexed on a tetragonal lattice with a=b=101.7Å, c=178.8Å in **I** and a=b=91.7Å, c=159.8Å in **II**. The d-spacings and indices are listed in Tables S1 and S2 of Supporting Information (SI). The extinction rule observed agrees with $I4_122$ symmetry, as previously determined. Note that most peaks have indices (in black) with both h+k and l even. If only such peaks were present, the diffraction pattern could be indexed to a smaller, also tetragonal unit cell, with $a'=b'=a/\sqrt{2}$, and $c'=c/2$, with symmetry $P4_222$ (green). In our powder pattern there is one peak that can only be indexed as (303) of the $I4_122$ lattice. Other non-$P4_222$ peaks may also be present, but most of them coincide with some $P4_222$ peaks (Fig. 2b). Previously it was only by single crystal diffraction that the SmQ space group was determined as $I4_122$.[12] The weakness of the non-$P4_222$ peaks suggests, however, that the $I4_122$ structure of SmQ is probably a slightly modified/distorted $P4_222$, a starting point for our next step in determining the SmQ structure.

Using the intensities of the six strongest diffraction peaks of compound **II**, we are able to reconstruct candidate electron density (ρ) maps of the SmQ phase, with different combinations of phase angles. Among the six strongest peaks, two can have alternative (*hkl*) indexing, i.e. (200) or (103) and (202) or (211). We took the assumption that $P4_222$ peaks are much stronger than non-$P4_222$ ones, and attributed the intensity of the two peaks to (200) and (202) respectively. As a consequence the reconstructed ρ-maps, even though using $I4_122$ lattice symmetry, in fact consist of four unit cells of $P4_222$ space group (Fig. 3a).

The selected 3D ρ-map (Fig. 3a, for details see SI) shows the high-ρ regions of the unit cell (55% of the total volume) occupied by the aromatic cores. It is evident from the map that the structure consists of columns. In the full cell there are four of them along *x*, four along *y* and two along *z*. Molecular assembly into columns is in line with the fact that in the phase diagram SmQ is close to Cub/$Ia\bar{3}d$, which itself consists of columnar segments. The arrangement of horizontal columns bears strong resemblance to that proposed by Pansu et al.,[12] even though in their model smectic blocks were assumed instead of columns.

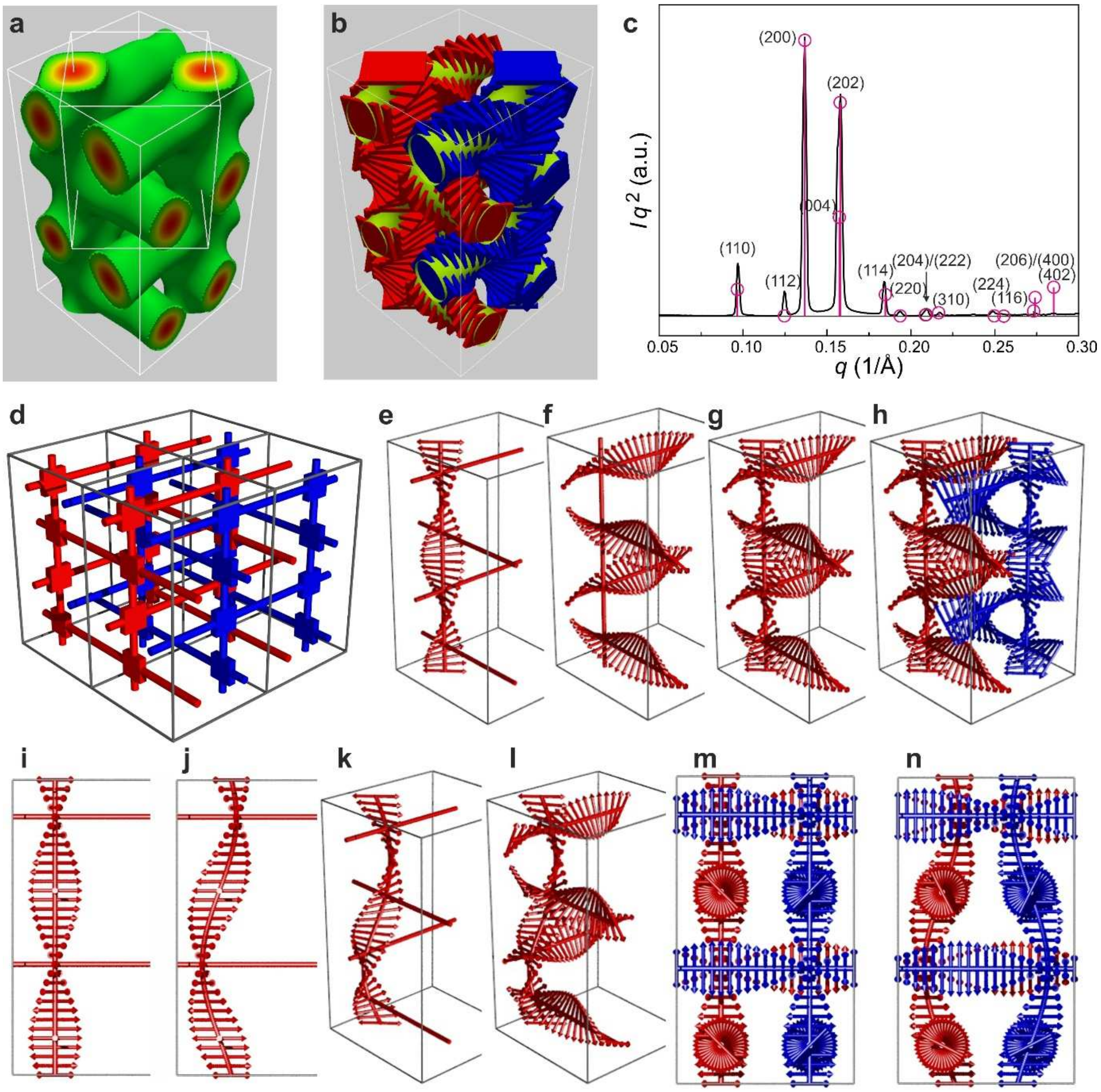

Figure 3. Results of X-ray analysis and structure of the SmQ. (a) Electron density (ρ) map (compound **II**, 155℃) , showing the high-to-medium ρ regions in the unit cell (red = high, green = medium, none = low). The large (true) cell corresponds to $I4_122$, while the small approximant cell has $P4_222$ symmetry, and contains ¼ of the full cell volume. (b) Geometric model, superimposed on the map in (a), used to simulate the diffraction pattern, where helical columns consist of stacked solid plates representing the strata consisting of ~4 molecular cores lying side-by-side normal to column axis (*cf*. Fig. 4c). (c) Comparison of experimental X-ray diffractogram and that simulated from the model in (b) (red vertical lines topped by circles). (d) Double network representation of the SmQ structure, with planar four-way junctions (2x2 unit cells). (e-h) The helicity of the columns is generated by rotation of the molecular strata, each represented by a double arrow, about the column axis. Within a cell, a stratum rotates by 360° along a vertical column (e), and by 180° along a horizontal column (f). The two networks have the same helical sense (g-h). Distortion of the vertical column from a 4_2 (i) to a 4_1 helix (j-l).

(m) View along [100] on the complete structure with $P4_222$ symmetry (2 cells) and (n) $I4_122$ symmetry (1 cell). (Full page width)

According to the 3D ρ map, in the SmQ structure there are layers of horizontal columns aligned, alternatively, along *x* and *y*. There are also two vertical columns in a unit cell, each intersecting with four horizontal columns. The resulting periodic structure consists of two infinite interpenetrating networks of columns with planar 4-way junctions (Fig. 3d). The two networks are related by a shift of (1/2,1/2,1/2). Each junction joins four segments, two horizontal and two vertical. For compound **II,** the length of the horizontal segments between junctions is *a*=91.7Å, and between vertical segment *c*/4=40.0Å. The distance between columns matches well with the extended molecular length of 46Å.The four segments at a junction are always within a vertical plane, and we expect the molecules near the junction to orient mainly perpendicular to that plane. At successive junctions along a horizontal column, the molecular orientation is the same, while along a vertical segment it is rotated by 90°.

As has been hypothesised before for bicontinuous $Ia\bar{3}d$ and triple-network cubic phases formed by rod-like molecules,[17,21] the columnar segments consist of stacked layers (strata) of several molecules lying side-by-side. The columns are helical[17] because successive strata rotate about the column axis to avoid steric clash between pendant chains. We postulate similar twisted columns in the SmQ phase (Fig. 3). It is estimated that the strata contain 4 molecules each, and are rotated by 8.9° and 10.2° relative to their neighbours in the horizontal and vertical columns, respectively (see SI). For comparison in the Cub/$Ia\bar{3}d$ in compound **II**, the rotation angle is 8.4°. Had the twist between strata been the same in horizontal and vertical segments, the length of the former would have been twice that of the latter, and the *c/a* ratio would have been 2 instead of the observed 1.74. The fact that horizontal segments are slightly longer than half the vertical segments can be explained by the planar junctions, all of them vertical, having finite thickness. Close to the junction, the twist of the strata in all four adjoining branches would cause a clash, which can be resolved by some spreading of the junction area in a horizontal direction.

As already proposed for the bicontinuous $Ia\bar{3}d$ and triple-network cubic phases,[17] to minimize the clash between columns at a junction and allow their smooth merger, all converging columns should possess the same chirality. This then allows long-range propagation of homochirality throughout the network. Furthermore, the body-centred symmetry $I4_122$ mandates that the two networks in the SmQ be exactly the same apart from a shift by (1/2,1/2,1/2). Accordingly, both networks are chiral and of the same handedness, which results in net chirality of the phase, and explains why it had previously been found only in enantiopure chiral compounds: molecules of wrong intrinsic chirality will destabilize the phase.

Based on the above, we are able to construct a geometrical model of the SmQ phase and to simulate its diffraction pattern. The geometric model is shown in Fig.

3b, where the high-ρ core of each molecular stratum is represented by a platelet, whose length should be that of the molecular core, and width depends on the number of molecules in the stratum. Using the length l and width w of the plates as the fitting parameters, a very good fit between simulated and experimental patterns is achieved as shown in Fig. 3c. The best-fit parameters are l=31.4Å and w=29.0Å, agreeing reasonably well with estimation (30Å and 25Å) on the basis of molecular size, cell dimensions and density estimation.

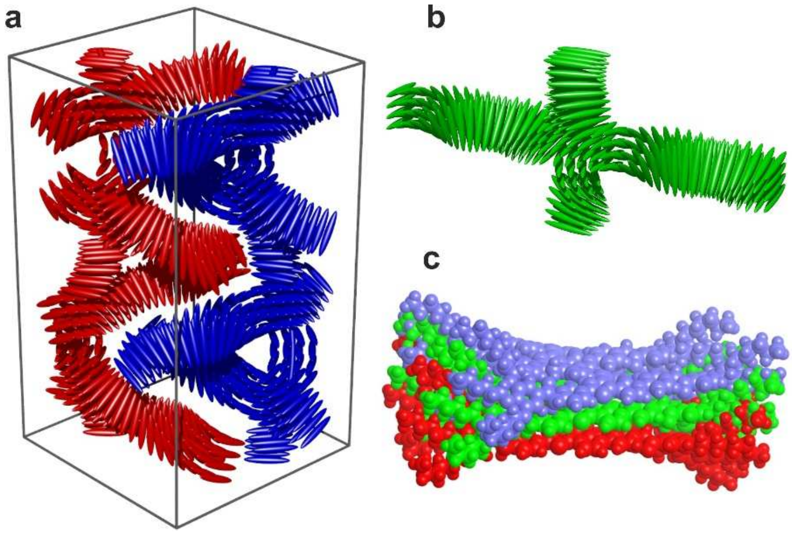

Figure 4. Twisted networks and molecules. (a) Perspective view of an $I4_122$ SmQ unit cell – see video of full 360° rotation of the model in SI. (b) Converging columns at junctions possess the same chirality to avoid clashes. (c) Model of three successive strata, each containing four molecules of **I**, with interstrata spacing of 4.5 Å and an 8° twist. Each stratum is represented by four rigid rods in (A, B).

However, the true space group of the structure is $I4_122$, as established by single crystal X-ray study before,[12] and supported by the observation of non-$P4_222$ reflections in our powder diffractograms. The reduction in symmetry from $P4_222$ to $I4_122$ can be explained as follows. The helical symmetry of the vertical columns will be reduced from 4_2 to 4_1 if the centres of the molecular strata are shifted off-axis. They then follow a helical path (Fig. 3i,j). The junction points and the horizontal columns are similarly shifted in different directions at different heights (Fig. 3k,l,n), resulting in $I4_122$ lattice symmetry. This sideway shift is small though, since our diffraction pattern simulation suggests that for large distortions many unobserved $I4_122$ peaks, such as (101), would become visible. A perspective view of the full $I4_122$ unit cell (with an exaggerated distortion) is shown in Fig.4a.

The current model of the SmQ phase is also able to explain its extremely low birefringence Δn. The Δn is expected to be ~0.004 because, while the horizontal columns contribute positive birefringence, the vertical ones add negative (Supporting Information). This estimate is in good agreement with the previously reported Δn value of < 0.005,[12] and our own measurement of ~0.004 (SI).

As mentioned, we propose that the molecular twist is caused by steric clash between pendant chains on successive strata, as shown in the molecular model of three overlaying strata in Fig. 4c. The likely propeller-like chiral conformation of an individual molecule is due to the non-planarity of the ester groups, with a racemization barrier of E^*=2.6 kJ/mol.[19] The twist angle between the successive strata is a compromise between the steric avoidance of the bulky aliphatic chains and the tendency for maximum overlap of the aromatic cores. In accordance with the general principle of chirality synchronization by dense self-assembly,[22- 25] the close packing requires a coordinated flip of many (n) molecules to change chirality, which raises the effective helix inversion barrier to a prohibitive value of nE^*.

What the observed phase behaviour demonstrates clearly is that any phase transition that involves helix inversion is highly suppressed. This explains the suppression of the Iso$^{[*]}$ – Cub/$Ia\bar{3}d$ transition, which either proceeds via SmQ (in **I**) or shows a large, nearly 30 K, hysteresis (in **II**). Since Cub/$Ia\bar{3}d$ consists of two networks of opposite chirality, to grow one of them from a dense homochiral environment requires helix inversion. Similar suppression of helix inversion is responsible for the triangular shape of Cub/$Ia\bar{3}d$ domains growing from the homochiral SmQ (Fig. 1c,d). Interestingly, it was also observed that when Cub/$Ia\bar{3}d$ grows from the Iso$^{[*]}$ liquid, its domains nucleate exclusively at boundaries between enantiomeric Iso$^{[*]}$ domains[19] where both helical hands are available; this indicates that helix inversion presents a particularly high barrier in the nucleation process. The strong suppression of nucleation and growth of Cub/$Ia\bar{3}d$ domains from Iso$^{[*]}$ also suggests that Iso$^{[*]}$ liquid may also consist of densely packed homochiral helical segments, albeit with only short-range positional order.

There is an interesting analogy between the structure of SmQ and those of “blue phases” BPI and BPII,[26] two variants of chiral nematic with an ordered array of double-twist defect lines observed in highly chiral LCs. Although BP structures are on micro- and SmQ on nanoscale, both types involve orthogonal packing of helices.

The unusual structure of SmQ also makes it a good candidate for applications such as in circularly polarized light (CPL) emitters. There is no need of alignment as the structure is almost isotropic, and no need for complex asymmetric synthesis, as only a minute admixture of chiral dopant achieves macroscopic homochirality of the required sense.[24] Direct CPL emission would cut the need for filters e.g. in an AMOLED display, and halve the enegy consumption. CPL emitters, sensors and manipulators are also essential in optical communication,[27] quantum-based optical computing,[28] and as efficient LC display backlights.[29] Finally, the long-range chirality synchronization in SmQ, as well as in Iso$^{[*]}$ liquid and the triple network cubic phase, all occurring in achiral compounds, may also provide new insight into how homochirality could have propagated at the beginning of life on Earth.[30]

Acknowledgement

For help with synchrotron SAXS experiments we thank Nick Terrill and Olga Shebanova at I22, Diamond Light Source. We acknowledge financial support from EPSRC (EP-K034308, EP-P002250), DFG (TS 39/21-2), China Scholarship Council (HL) and Foreign Experts Program of PR China (GU).

References

---

[1] J. M. Seddon, *Biochemistry* **1990***, 29*, 7997-8002.

[2] A. J. Meuler, M. A. Hillmyer, F. S. Bates, *Macromolecules* **2009**, *42*, 7221–7250.

[3] G. Ungar, Y. Liu, X. B. Zeng, V. Percec, W.-D. Cho, *Science* **2003**, *299*, 1208-1211.

[4] X. B. Zeng, Y. Liu, G. Ungar, V. Percec, A. E. Dulcey, J. K. Hobbs, *Nature* **2004**, *428*, 157-160.

[5] S.-W. Lee, M. J. Bluemle, F. S. Bates, *Science* **2010**, *330*, 349-353.

[6] T. M. Gillard, S.-W. Lee, F. S. Bates, *PNAS* **2016**, *113*, 5167–5172.

[7] K. Hayashida, T. Dotera, A. Takano, Y. Matsushita, *Phys. Rev. Lett.* **2007**, *98*, 195502.

[8] S. A. Kim, K. J. Jeong, A. Yethiraj, M. K. Mahanthappa, *PNAS* **2017**, *114*, 4072-4077.

[9] C. H. Xiao, N. Fujita, K. Miyasaka, Y. Sakamoto, O. Terasaki, *Nature* **2012**, *487*, 349-353.

[10] A. M. Levelut, C. Germain, P. Keller, L. Liebert, J. Billard, *J. Physique,* **1983**, *44*, 623-629.

[11] A. M. Levelut, E. Hallouin, D. Bennemann, G. Heppke, D. Loetzsch, *J. Physique II France* **1997**, *7*, 981-1000.

[12] B. Pansu, Y. Nastishin, M. Imperor-Clerc, M. Veber, H. T. Nguyen, *Eur. Phys. J. E* **2004**, *15*, 225-230.

[13] M. Vogrin, N. Vaupotic, M. M. Wojcik, J. Mieczkowski, K. Madrak, D. Pociecha, E. Gorecka, *Phys. Chem. Chem. Phys*. **2014**, *16*, 16067-16074.

[14] M. Yoneya, *Chem. Rec.* **2011**, *11*, 66-76.

[15] A. M. Levelut, M. Clerc, *Liq. Cryst*. **1998**, *24*, 105–115.

[16] X. B. Zeng, G. Ungar, M. Imperor-Clerc, *Nat. Mater.* **2005**, *4*, 562-567.

[17] C. Dressel, F. Liu, M. Prehm, X. B. Zeng, G. Ungar, C. Tschierske, *Angew. Chem. Int. Ed*. **2014**, *126*, 13331-13336.

[18] T. Yamamoto, I. Nishiyama, M. Yoneya, H. Yokoyama, *J. Phys. Chem. B* **2009**, *113*, 11564–11567.

[19] C. Dressel, T. Reppe, M. Prehm, M. Brautzsch, C. Tschierske, *Nat. Chem*. **2014**, *6*, 971-977.

[20] T. Okihara, L. Cartier, G. O. R. Alberda van Ekenstein, B. Lotz, *Polymer* **1998**, *40*, 1-11.

[21] M. Gharbi, A. Gharbi, H. T. Nguyen, J. Malthete, *Curr. Opin. Colloid Interface Sci*. **2002**, *7*, 312-325.

[22] M. M. Green, J. M. Park, T. Sato, A. Teramoto, S. Lifson, R. L. B. Selinger, J. V. Selinger, *Angew. Chem. Int. Ed.* **1999**, *38*, 3138-3154.

[23] J. Malthete, A. Collet, *J. Am. Chem. Soc.* **1987**, *109*, 7544-7545.

[24] C. Tschierske, G. Ungar, *ChemPhysChem* **2016**, *17*, 9-26.

[25] E. Yashima, N. Ousaka, D. Taura, K. Shimomura, T. Ikai, K. Maeda, K. *Chem. Rev.* **2016**, *116*, 13752−13990.

[26] D. C. Wright, N. D. Mermin, *Rev. Mod. Phys*. **1989**, *61*, 385–432.

[27] R. Farshchi, M. Ramsteiner, J. Herfort, A. Tahraoui, H. T. Grahn, *Appl Phys Lett.* **2011**, *98*, 162508.

[28] J. F. Sherson, H. Krauter, R. K. Olsson, B. Julsgaard, K. Hammerer, I. Cirac, E. S. Polzik, *Nature* **2006**, *443*, 557-560.

[29] M. Schadt, *Annu Rev Mater Sci* **1997**, *27*, 305-379.

[30] M. M. Green, V. Jain, *Origin Life Evol. Biosph*. **2010**, *40*, 111-118.